Hyperintense signal on diffusion-weighted imaging for monitoring the acute response and local recurrence after photodynamic therapy in malignant gliomas

Fujita, Yuichi ; Nagashima, Hiroaki ; Tanaka, Kazuhiro ; Hashiguchi, Mitsuru ; Itoh, Tomoo ; Sasayama, Takashi

(Citation)
Journal of Neuro-Oncology,155(1):81-92

(Issue Date)
2021-10-30

(Resource Type)
journal article

(Version)
Accepted Manuscript

(URL)
https://hdl.handle.net/20.500.14094/90008719

Hyperintense signal on diffusion-weighted imaging for monitoring the acute response and local recurrence after photodynamic therapy in malignant gliomas

Yuichi Fujita[1], Hiroaki Nagashima[1], Kazuhiro Tanaka[1], Mitsuru Hashiguchi[1], Tomoo Itoh[2], Takashi Sasayama[1]

[1]Department of Neurosurgery, Kobe University Graduate School of Medicine, Kobe, Hyogo, Japan

[2]Department of Diagnostic Pathology, Kobe University Graduate School of Medicine, Kobe, Hyogo, Japan

*Corresponding author: Yuichi Fujita

Department of Neurosurgery, Kobe University Graduate School of Medicine

7-5-1 Kusunoki-cho, Chuo-ku, Kobe, Hyogo 650-0017, Japan

Phone: +81-78-382-5966; Fax: +81-78-382-5979

E-mail: fyuichi@med.kobe-u.ac.jp

ORCID: 0000-0002-1944-0925

Abstract

Purpose: Photodynamic therapy (PDT) subsequent to surgical tumor removal is a novel localized treatment for malignant glioma that provides effective local control. The acute response of malignant glioma to PDT can be detected as linear transient hyperintense signal on diffusion-weighted imaging (DWI) and a decline in apparent diffusion coefficient (ADC) values without symptoms. However, their long-term clinical significance has not yet been examined. The aim of this study was to clarify the link between hyperintense signal on DWI as an acute response and recurrence after PDT in malignant glioma.

Methods: Thirty patients (16 men; median age, 60.5 years) underwent PDT for malignant glioma at our institution between 2017 and 2020. We analyzed the signal changes on DWI after PDT and the relationship between these findings and the recurrence pattern.

Results: All patients showed linear hyperintense signal on DWI at the surface of the resected cavity from day 1 after PDT. These changes disappeared in about 30 days without any neurological deterioration. During a mean post-PDT follow-up of 14.3 months, 19 patients (63%) exhibited recurrence: 10 local, 1 distant, and 8 disseminated. All of the local recurrences arose from areas that did not show hyperintense signal on DWI obtained on day 1 after PDT.

Conclusion: The local recurrence in malignant glioma after PDT occurs in an area without hyperintense signal on DWI as an acute response to PDT. This characteristic finding could aid in the monitoring of local recurrence after PDT.

Keywords: glioma; glioblastoma; photodynamic therapy; recurrence; diffusion-weighted imaging

List of Abbreviations

ADC, apparent diffusion coefficient

CE-T1WI, contrast-enhanced T1-weighted imaging

DWI, diffusion-weighted imaging

FLAIR, fluid-attenuated inversion recovery

FOV, field of view

IDH, isocitrate dehydrogenase

MGMT, O^6-methylguanine-DNA methyltransferase

MR, magnetic resonance

PDT, photodynamic therapy

TE, echo time

TI, inversion time

TR, repetition time

WHO, World Health Organization

Introduction

Survival is associated with the extent of resection in patients with glioblastoma, the most aggressive primary malignant brain tumor [1-4]. However, optimal surgical treatment that balances maximal resection and safe resection is still challenging in glioblastoma because of its incredibly invasive nature [5]. Standard therapy includes maximal possible surgical resection followed by radiotherapy and concomitant temozolomide-based chemotherapy and often leads to local recurrence [6-10]. Photodynamic therapy (PDT) subsequent to surgical tumor removal is a novel localized treatment for malignant glioma and a possible alternative to standard therapy. PDT is a light-activated treatment modality that provides effective local control [11-13]. In PDT, a photosensitizer that is intravenously injected before surgery and selectively accumulates in the tumor is transformed from its ground state into an electronically excited state by semiconductor laser of a specific wavelength; this transfers the energy directly to triplet oxygen to form singlet oxygen (a type II reaction), which exerts an antitumor effect specifically in tumor cells while preserving the surrounding normal brain cells [14-16]. However, even PDT cannot completely suppress local recurrence [11, 12].

The treatment outcome of glioblastoma at recurrence is devastating with all known types of therapy [17] but second surgery to treat recurrence is considered a valid option [18-22]. Reoperation in selected patients with a favorable Karnofsky Performance Status (KPS) score at the time of recurrence significantly improves overall survival from recurrence without a significant decrease in functional status [21, 22]. To enable second surgery as a treatment option for recurrence, the early detection of the resectable recurrence before the patient's KPS score decreases is crucial.

We previously reported that the acute response of malignant glioma to PDT can be detected as transient linear hyperintense signal on diffusion-weighted imaging (DWI) and a decline in apparent diffusion coefficient (ADC) values without symptoms [23]. However, the long-term clinical significance of these imaging findings was not examined. Outcomes would be improved if recurrence could be predicted earlier from this characteristic PDT-induced change on magnetic resonance (MR) images. We hypothesized that the characteristic hyperintense signal on DWI could help not only to confirm the PDT-irradiated area, but also to monitor the local recurrence site after PDT in malignant glioma. The aim of this study was to clarify the link between hyperintense signal on DWI as an acute response and recurrence after PDT in malignant glioma.

Methods

Study design

This study was approved by the institutional review board (protocol number B190100) and conducted according to institutional and national ethical guidelines and in accordance with the Helsinki Declaration.

At our institution, PDT has been combined with conventional surgery since August 2017. The target patients for PDT are those with confirmed World Health Organization (WHO) grade III or IV glioma by rapid intraoperative pathological diagnosis and those who underwent more than 90% (gross total or subtotal) resection of contrast-enhancing lesions or intentional partial resection due to involvement of eloquent areas. Thirty consecutive patients underwent PDT for malignant glioma at our institution between August 2017 and December 2020. We analyzed the signal changes on DWI after PDT and the link between these findings and the recurrence pattern.

PDT procedure

(1) Preoperative: Patients preoperatively expected to have a higher-grade glioma were scheduled for PDT. These patients were administered a single intravenous injection of talaporfin sodium (Laserphyrin; Meiji Seika Pharma Co., Ltd., Tokyo, Japan) at a dose of 40 mg/m^2 22–26 h before surgery.

(2) Intraoperative: The histological malignancy (WHO grade III or higher) was confirmed by rapid intraoperative pathological diagnosis. After maximum resection of the contrast-enhancing lesion, complete hemostasis was ensured before PDT irradiation. Next, the entire resection cavity was irradiated with a 664-nm semiconductor laser (Meiji Seika Pharma Co., Ltd.) (diameter, 1.5 cm; radiation power density, 150 mW/cm^2; radiation energy density, 27 J/cm^2). Each irradiation was performed for 3 minutes per spot without overlap. The large blood vessels were protected by aluminum foil to avoid their direct irradiation (Supplementary Fig. 1).

(3) Postoperative: For the prevention of photosensitive dermatosis, post-therapeutic light protection (<500 lx) was performed for 10–14 days.

As post-PDT therapy, radiotherapy plus concomitant and adjuvant temozolomide (Stupp regimen) were typically started as soon as the final histological and molecular/genetic integrated diagnosis was confirmed.

Imaging analysis

Post-PDT imaging follow-up was performed using a 3.0-T MR imaging scanner (Achieva; Philips Medical Systems, Eindhoven, The Netherlands) on days 1, 7, 14, 30, and 60 and every 3 months after that. Extra MR imaging was performed at the time of neurological deterioration. Conventional MR imaging sequences included DWI (b-values, 0 and 1000 s/mm^2; repetition time [TR]/echo time [TE], 4500/75 ms; field of view [FOV], 240

mm; slice thickness, 4 mm; slice gap, 1 mm; matrix, 109 × 128; flip angle, 90°); T2-weighted imaging (TR/TE, 4200/100 ms; FOV, 230 mm; matrix, 320 × 400; slice thickness, 5.0 mm); T2-weighted fluid-attenuated inversion recovery (FLAIR; TR/TE/inversion time [TI], 11000/125/2800 ms; FOV, 230 mm; matrix, 204 × 256; slice thickness, 5.0 mm); and three-dimensional T1-weighted imaging (TR/TE, 5.0/2.2 ms; FOV, 240 mm; matrix, 304 × 304; slice thickness, 0.8 mm) before and after injection of intravenous gadolinium contrast agent (0.2 ml/kg; Magnescope, Guerbet, Paris, France). In this study, recurrence was defined as follows: local recurrence, growth of a contrast-enhancing lesion at the primary tumor bed; distant recurrence, growth of a contrast-enhancing lesion that appeared separately from the primary tumor bed; dissemination, arachnoid or ependymal enhancement away from the primary tumor site or spinal metastasis. To distinguish between recurrence and pseudoprogression, we also defined pseudoprogression according to the Response Assessment in Neuro-Oncology criteria as follow: new or enlarging contrast-enhancing lesion occurring within 12 weeks after the completion of radiotherapy in the absence of true progressive disease. Recurrence was assessed by two independent reviewers (KT and TS). The link between the signal changes on DWI obtained on day 1 after PDT and the recurrence site was analyzed by three independent reviewers (YF, HN, and TS).

Statistical analysis

The characteristics of recurrent and non-recurrent patients were compared using Fisher's exact test and the Mann–Whitney U test. The Kruskal-Wallis test with the Steel-Dwass post hoc test was used to compare the characteristics of patients based on recurrence patterns. All statistical analyses were performed with EZR (Saitama Medical Center, Jichi Medical University, Saitama, Japan), which is a graphical user interface for R software (http://www.r-project.org/) [24]. A two-sided p-value < 0.05 was considered statistically significant.

Results

Patient characteristics

In total, 30 patients were included in the study. Their characteristics are summarized in Table 1. They comprised 16 men (53%) and 14 women (47%) with a median age of 60.5 (range, 23–85) years and median preoperative KPS score of 80 (range, 30–100). Of the 30 tumors, 14 (47%) were located in the frontal lobe, 9 (30%) in the temporal lobe, 4 (13%) in the parietal lobe, 1 (3%) in the occipital lobe, 1 (3%) in the insula, and 1 (3%) in the basal ganglia. In addition, 20 tumors (67%) were in the right cerebral hemisphere and 10 (33%) in the left. The median preoperative tumor volume was 32.9 cm^3 (range, 2.2–140.0 cm^3). Gross total resection (extent of

resection, > 95%) was achieved in 23 patients (77%), subtotal resection (extent of resection, 90–95%) in 5 (17%), and partial resection (extent of resection, 50–90%) in 2 (7%). The median number of PDT irradiation spots was 14 (range, 2–31). There were no PDT-related complications including photosensitive dermatosis and infection. WHO grade III glioma (anaplastic astrocytoma and anaplastic oligodendroglioma) was histologically verified in 4 patients (13%), with grade IV glioma (glioblastoma) in 26 (87%). Isocitrate dehydrogenase (IDH) mutation was verified in 5 patients (17%). O^6-methylguanine-DNA methyltransferase (MGMT) promoter methylation was verified in 15 patients (50%). Postoperatively, all patients underwent radiotherapy and concomitant temozolomide-based chemotherapy. One patient was allergic to temozolomide and was switched to the procarbazine, 1-[(4-amino-2-methyl-5-pyrimidinyl) methyl]-3-(2-chloroethyl)-3-nitrosourea (ACNU), and vincristine (PAV) regimen. Eight patients were treated with combined bevacizumab and temozolomide as first-line chemotherapy and 3 patients underwent tumor-treating fields therapy.

Recurrence after PDT

Of the 30 patients, 19 (63%) exhibited recurrence—local recurrence in 10 (33%), distant recurrence in 1 (3%), and dissemination in 8 (27%)—during a median follow-up period of 14.3 (range, 3.4–45.9) months. The tumor characteristics based on the recurrence pattern after PDT are summarized in Table 2. There was no significant difference in the baseline characteristics between recurrent and non-recurrent patients, except for the higher MIB-1 index in the recurrent patients (Supplementary Table 1). There was also no significant difference in the patient characteristics between the recurrence patterns (Supplementary Table 2).

Post-PDT MR imaging

In all patients, linear hyperintense signals on DWI were detected at the surface of the resected cavity from day 1 after PDT (Figs. 1–4). All hyperintense signals on DWI disappeared in about 30 days without any neurological deterioration (Supplementary Fig. 2).

All local recurrences arose from areas that did not show a hyperintense signal on DWI obtained on day 1 after PDT (Figs. 1 and 2). Patients with distant recurrence or dissemination tended to have uninterrupted hyperintense signal on DWI obtained on day 1 after PDT (Figs. 3 and 4). No patient exhibited pseudoprogression.

Illustrative local recurrence cases

Case 1. A 49-year-old right-handed woman presented with episodes of convulsive seizures. Preoperative MR imaging revealed a contrast-enhancing mass lesion with a necrotic area in the left frontal lobe (tumor volume, 17.8 cm^3) (Fig. 1a, upper row). Awake surgery was performed because the tumor was close to Broca's area. Gross total resection of the contrast-enhancing lesion was achieved without aphasia. After the histological malignancy was confirmed in rapid intraoperative pathological diagnosis, PDT was performed (irradiation spots, 11). Postoperative MR images obtained on day 1 after PDT showed complete resection and hyperintense signal on DWI adjacent to the resection cavity wall without symptoms (Fig. 1a, middle row). The final histological and molecular/genetic integrated diagnosis was WHO grade IV glioblastoma, IDH wild-type. She underwent radiotherapy, concomitant and adjuvant temozolomide, and tumor-treating fields therapy. However, she was found to be allergic to temozolomide in one cycle of adjuvant temozolomide and was switched to the PAV regimen. After three cycles of the PAV regimen, her chemotherapy was switched to bevacizumab alone due to paralytic ileus, an adverse effect of vincristine. Eventually, she exhibited local recurrence 22.5 months after surgery (Fig. 1a, lower row). The recurrence site was the area that did not show a hyperintense signal on DWI obtained on day 1 after PDT (Fig. 1b). She continued bevacizumab and tumor-treating fields therapy for the recurrence and had a good KPS score (90) 5.5 months after recurrence at final follow-up.

Case 2. A 67-year-old right-handed woman presented with headache and left homonymous hemianopia. Preoperative MR images revealed a ring-enhancing mass lesion in the right temporal lobe (tumor volume, 60.6 cm^3) (Fig. 2a, upper row). After the histological malignancy was confirmed in rapid intraoperative pathological diagnosis, the contrast-enhancing lesion was completely resected and PDT was performed (irradiation spots, 29). Postoperative MR images obtained on day 1 after PDT showed complete resection and hyperintense signal on DWI adjacent to the resection cavity wall without symptoms (Fig. 2a, middle row). The final histological and molecular/genetic integrated diagnosis was WHO grade IV glioblastoma, IDH wild-type. She underwent radiotherapy, concomitant and adjuvant temozolomide, and tumor-treating fields therapy. Eventually, she exhibited local recurrence 7.7 months after surgery (Fig. 2a, lower row). The recurrence site was the area that did not show a hyperintense signal on DWI obtained on day 1 after PDT (Fig. 2b). She continued adjuvant temozolomide and tumor-treating fields therapy for the recurrence and had a good KPS score (70) 15.0 months after recurrence at final follow-up.

Discussion

Recurrence is a hallmark of malignant glioma, regardless of the therapy applied [6-10, 17]. Although PDT is a novel localized treatment for malignant glioma that can selectively kill tumor cells [14-16], it cannot completely prevent local recurrence [11, 12]. The prognosis of malignant glioma is unfortunately poor at recurrence, but its early detection can vastly improve the clinical course and patients' management, such as reoperation, which might boost prognosis [18-22]. In this study, we found that a hyperintense signal on DWI as the post-PDT acute response helped to predict the local recurrence site. The PDT-irradiated area asymptomatically showed transient linear hyperintense signal on DWI. All local recurrences arose from the areas without this hyperintense signal on DWI that did not show the acute response on day 1 after PDT.

PDT exploits the tumor-selective accumulation of a photosensitizer and a photochemical reaction upon semiconductor laser irradiation. In this study, talaporfin sodium, a second-generation photosensitizer, was used for PDT without the combination of other photosensitizers including 5-aminolevulinic acid. Singlet oxygen is generated and exerts an antitumor effect in the penetration depth of the semiconductor laser (5–7 mm) [11, 14]. The singlet oxygen exerts this antitumor effect without bystander effects because of its short migration distance (0.02–1 μm) and short lifetime (0.04–4 μs) [14, 25, 26]. Histopathologically, the effect of PDT is underpinned by direct tumor cell killing, including both apoptosis and necrosis [13, 27], tumor-associated vascular damage [28, 29], and activation of the immune response against tumor cells [30-32]. Because the PDT-induced cell damage and microcirculatory impairment leads to restricted diffusivity of water molecules, the PDT-irradiated area shows hyperintense signal on DWI and a decline in ADC values as the acute response [33]. All patients in this study exhibited linear hyperintense signal of about 5 mm in size on DWI at the surface of the resected cavity from day 1 after PDT, as we previously reported [23]. These characteristic changes asymptomatically disappeared in about 30 days.

About 80% of glioblastomas treated with the Stupp regimen develop local recurrence within 2 cm of the tumor margin [6-10, 17]. The extent of the glioblastoma resection is undoubtedly an independent prognostic factor [1-4]. However, Ellingson et al. reported that the postoperative residual contrast-enhancing tumor volume rather than extent of resection was a significant independent prognostic factor [34]. In line with this theory, PDT was added to maximal resection to kill as many tumor cells as possible around the resected cavity. PDT was a significant prognostic factor for overall survival and local progression-free survival [11, 12]. Nitta et al. reported that PDT provided effective local control (local recurrence rate, 33%) and led to increased relative rates of distant recurrence or dissemination [11]. In our study, local recurrence was observed in only 33% of patients, indicating excellent local control, as in Nitta et al. However, PDT cannot completely control local recurrence,

and the cause of PDT failure remains unclear. As a rule, we performed PDT irradiation avoiding the large blood vessels. Therefore, PDT non-irradiated area intentionally occurred. However, except for the intentional PDT non-irradiated area, the area that did not show a hyperintense signal on DWI obtained on day 1 despite PDT irradiation would be considered as a failure spot of PDT. Several factors have been reported to contribute to PDT resistance, including overexpression of antioxidant enzyme, activation of drug efflux pumps, degeneration of photosensitizer, and increased DNA repair capacity in glioblastoma cells [35-39]. Our findings suggest that local recurrence after PDT occurred from the area with no acute response to PDT. This evidence supports the belief that PDT is locally effective in areas with an acute response on DWI. Clarification of the relationship between the area without an acute response to PDT and resistance to PDT would be an issue for future studies aimed at reducing PDT failure.

The acute response of malignant gliomas to PDT was detected as asymptomatic transient linear hyperintense signal on DWI. Interestingly, all local recurrences after PDT occurred from areas that did not show a hyperintense signal on DWI obtained on day 1 after PDT. This characteristic finding could help to predict the local recurrence site. Careful observation of the areas without hyperintense signal on DWI after PDT might have a potential to support other MR imaging including FLAIR and contrast-enhanced T1-weighted imaging to detect progression. This would allow us to provide patients with greater opportunities for reoperation for resectable recurrence, which would undoubtedly improve their prognosis. At the same time, elucidation of the cause of PDT failure would be a key to further improve their prognosis.

Nonetheless, our study also has several limitations. First, the study was conducted at a single institution. Second, the number of patients was small. However, the safety and effectiveness of PDT in our study was almost the same as in a phase II clinical trial and a previous report [11, 12]. Third, the image comparison after PDT and at recurrence had to manually consider the morphological changes in the brain. Several conformational changes in the surgical cavity made it hard to be confident that the area of local recurrence was the same area without hyperintense signal on DWI on day 1 after PDT. However, at present, there is no imaging technique to automatically adjust for the postoperative morphological changes and make a perfect one-to-one correspondence considering the time course. To make up for this limitation, we performed MR imaging evaluations more frequently than usual in this study. Postoperative MR imaging is usually performed once before and after radiotherapy. On the other hand, we performed post-PDT MR imaging follow-up at least three times (day 1, 7, 14) before radiotherapy, and at least one time during radiotherapy (day 30). Furthermore, based on careful following and observation of the morphological changes in the surgical cavity on all postoperative MR imaging,

we analyzed the link between the DWI hyperintensity site on day1 after PDT and the recurrence site. To fundamentally resolve this limitation, it would be desirable to innovate imaging technology that could track postoperative morphological changes in the brain. Fourth, we could not find a significant link between the hyperintense signal on DWI as an acute response after PDT and distant recurrence or dissemination. The patients with distant recurrence or dissemination tended to have an uninterrupted hyperintense signal on DWI obtained on day 1 after PDT. However, the difference was not clear enough to allow their discrimination from the local recurrence cases. Fifth, this study could not fully examine the impact of bevacizumab on post-PDT MR imaging. Bevacizumab generally has a beneficial effect on pseudoprogression [40]. We had no patient with pseudoprogression in this study. Utilizing bevacizumab as first-line chemotherapy in almost one-third of our patients might contribute to this result. Finally, this study could not fully examine other risk factors for recurrence in malignant glioma after PDT. The primary tumors of all disseminated cases were localized near the ventricles. Ventricle contact has been associated with poor outcomes [41], whereas subventricular zone contact has been associated with dissemination [42]. Ventricular entry during resection has been linked to dissemination [43], although the connection is controversial [44, 45]. We also could not sufficiently address other several confounding factors such as extent of resection, IDH status, and MGMT promoter methylation status, due to small number of patients. All these factors have a potential to impact recurrence after PDT. Therefore, further studies using larger groups of patients and including these factors are needed to validate the recurrence pattern after PDT.

Nevertheless, it was clinically important that the local recurrence in malignant gliomas after PDT occurred in the area without the hyperintense signal on DWI as an acute response to PDT. To our knowledge, this is the first study to show the usefulness of visually clear hyperintense signal on DWI in the monitoring of local recurrence after PDT in malignant glioma.

Conclusions

This study provides new evidence that the local recurrence in malignant gliomas after PDT occurs in areas without hyperintense signal on DWI as an acute response to PDT. The characteristic hyperintense signal on DWI could help in the monitoring of not only the acute response to PDT, but also the local recurrence after PDT.

Declarations

Funding: This work was supported in part by Grants-in-Aid for Scientific Research from the Japanese Ministry

of Education, Culture, Sports, Science, and Technology [grant number: 20K09369 to Takashi Sasayama and 20K09389 to Kazuhiro Tanaka]. The sponsor had no role in the study design; in the collection, analysis, or interpretation of data; in the writing of the report; or in the decision to submit the article for publication.

Conflict of interest: All authors declare that they have no conflict of interest.

Availability of data and material: The data in this study are available from the corresponding author on reasonable request.

Code availability: No software application or custom code was used in this study.

Authors' contributions: Conception and design: YF, TS. Collection and assembly of data: YF, HN, KT, MH, TI, TS. Analysis and interpretation of data: YF, HN, KT, TS. Drafting the article: YF. Reviewed submitted version of manuscript: all authors. Approved the final version of manuscript: all authors.

Ethics approval: The study was approved by the institutional review board (protocol number B190100) and conducted according to institutional and national ethical guidelines and in accordance with the Helsinki Declaration.

Consent to participate: Patient informed consents were waived by the institutional review board due to the retrospective nature of the study and use of anonymized data.

Consent for publication: Not applicable.

Acknowledgments: We thank Ms. Takiko Uno for molecular analysis of the IDH mutation status of the patients included in this study.

References

1. Sanai N, Polley MY, McDermott MW, Parsa AT, Berger MS (2011) An extent of resection threshold for newly diagnosed glioblastomas. J Neurosurg 115:3-8. https://doi.org/10.3171/2011.2.JNS10998
2. Marko NF, Weil RJ, Schroeder JL, Lang FF, Suki D, Sawaya RE (2014) Extent of resection of glioblastoma revisited: Personalized survival modeling facilitates more accurate survival prediction and supports a maximum-safe-resection approach to surgery. J Clin Oncol 32:774-782. https://doi.org/10.1200/JCO.2013.51.8886
3. Lacroix M, Abi-Said D, Fourney DR, Gokaslan ZL, Shi W, DeMonte F, Lang FF, McCutcheon IE, Hassenbusch SJ, Holland E, Hess K, Michael C, Miller D, Sawaya R (2001) A multivariate analysis of 416 patients with glioblastoma multiforme: Prognosis, extent of resection, and survival. J Neurosurg 95:190-198. https://doi.org/10.3171/jns.2001.95.2.0190
4. Grabowski MM, Recinos PF, Nowacki AS, Schroeder JL, Angelov L, Barnett GH, Vogelbaum MA (2014) Residual tumor volume versus extent of resection: Predictors of survival after surgery for glioblastoma. J Neurosurg 121:1115-1123. https://doi.org/10.3171/2014.7.JNS132449
5. Burger PC, Heinz ER, Shibata T, Kleihues P (1988) Topographic anatomy and CT correlations in the untreated glioblastoma multiforme. J Neurosurg 68:698-704. https://doi.org/10.3171/jns.1988.68.5.0698
6. Brandes AA, Tosoni A, Franceschi E, Sotti G, Frezza G, Amistà P, Morandi L, Spagnolli F, Ermani M (2009) Recurrence pattern after temozolomide concomitant with and adjuvant to radiotherapy in newly diagnosed patients with glioblastoma: Correlation with MGMT promoter methylation status. J Clin Oncol 27:1275-1279. https://doi.org/10.1200/JCO.2008.19.4969
7. Dörner L, Mustafa A, Rohr A, Mehdorn HM, Nabavi A (2013) Growth pattern of tumor recurrence following bis-chloroethylnitrosourea (BCNU) wafer implantation in malignant glioma. J Clin Neurosci 20:429-434. https://doi.org/10.1016/j.jocn.2012.01.060
8. Rapp M, Baernreuther J, Turowski B, Steiger H-J, Sabel M, Kamp MA (2017) Recurrence pattern analysis of primary glioblastoma. World Neurosurg 103:733-740. https://doi.org/10.1016/j.wneu.2017.04.053
9. Gaspar LE, Fisher BJ, Macdonald DR, LeBer DV, Halperin EC, Schold SC Jr, Cairncross JG (1992) Supratentorial malignant glioma: Patterns of recurrence and implications for external beam local treatment. Int J Radiat Oncol Biol Phys 24:55-57. https://doi.org/10.1016/0360-3016(92)91021-E
10. Konishi Y, Muragaki Y, Iseki H, Mitsuhashi N, Okada Y (2012) Patterns of intracranial glioblastoma recurrence after aggressive surgical resection and adjuvant management: retrospective analysis of 43 cases. Neurol Med Chir (Tokyo) 52:577-586. https://doi.org/10.2176/nmc.52.577
11. Nitta M, Muragaki Y, Maruyama T, Iseki H, Komori T, Ikuta S, Saito T, Yasuda T, Hosono J, Okamoto S, Koriyama S, Kawamata T (2018) Role of photodynamic therapy using talaporfin sodium and a semiconductor laser in patients with newly diagnosed glioblastoma. J Neurosurg 131:1361-1368. https://doi.org/10.3171/2018.7.JNS18422
12. Muragaki Y, Akimoto J, Maruyama T, Iseki H, Ikuta S, Nitta M, Maebayashi K, Saito T, Okada Y, Kaneko S, Matsumura A, Kuroiwa T, Karasawa K, Nakazato Y, Kayama T (2013) Phase II clinical

study on intraoperative photodynamic therapy with talaporfin sodium and semiconductor laser in patients with malignant brain tumors. J Neurosurg 119:845-852. https://doi.org/10.3171/2013.7.JNS13415

13. Akimoto J (2016) Photodynamic therapy for malignant brain tumors. Neurol Med Chir (Tokyo) 56:151-157. https://doi.org/10.2176/nmc.ra.2015-0296

14. Henderson BW, Dougherty TJ (1992) How does photodynamic therapy work? Photochem Photobiol 55:145-157. https://doi.org/10.1111/j.1751-1097.1992.tb04222.x

15. Dolmans EJGJ, Fukumura D, Jain RK (2003) Photodynamic therapy for cancer. Nat Rev Cancer 3:380-387. https://doi.org/10.1038/nrc1071

16. Castano AP, Mroz P, Hamblin MR (2006) Photodynamic therapy and anti-tumour immunity. Nat Rev Cancer 6:535-545. https://doi.org/10.1038/nrc1894

17. Stupp R, Mason WP, van den Bent MJ, Weller M, Fisher B, Taphoorn MJB, Belanger K, Brandes AA, Marosi C, Bogdahn U, Curschmann J, Janzer RC, Ludwin SK, Gorlia T, Allgeier A, Lacombe D, Cairncross JG, Eisenhauer E, Mirimanoff RO, European Organisation for Research and Treatment of Cancer Brain Tumor and Radiotherapy Groups; National Cancer Institute of Canada Clinical Trials Group (2005) Radiotherapy plus concomitant and adjuvant temozolomide for glioblastoma. N Engl J Med 352:987-996. https://doi.org/10.1056/NEJMoa043330

18. Azoulay M, Santos F, Shenouda G, Petrecca K, Oweida A, Guiot MC, Owen S, Panet-Raymond V, Souhami L, Abdulkarim BS (2017) Benefit of re-operation and salvage therapies for recurrent glioblastoma multiforme: results from a single institution. J Neurooncol 132:419-426. https://doi.org/10.1007/s11060-017-2383-2

19. Tully PA, Gogos AJ, Love C, Liew D, Drummond KJ, Morokoff AP (2016) Reoperation for recurrent glioblastoma and its association with survival benefit. Neurosurgery 79:678-689. https://doi.org/10.1227/NEU.0000000000001338

20. Suchorska B, Weller M, Tabatabai G, Senft C, Hau P, Sabel MC, Herrlinger U, Ketter R, Schlegel U, Marosi C, Reifenberger G, Wick W, Tonn JC, Wirsching H-G (2016) Complete resection of contrast-enhancing tumor volume is associated with improved survival in recurrent glioblastoma - Results from the DIRECTOR trial. Neuro Oncol 18:549-556. https://doi.org/10.1093/neuonc/nov326

21. Montemurro N, Perrini P, Blanco MO, Vannozzi R (2016) Second surgery for recurrent glioblastoma: A concise overview of the current literature. Clin Neurol Neurosurg 142:60-64. https://doi.org/10.1016/j.clineuro.2016.01.010

22. Wann A, Tully PA, Barnes EH, Lwin Z, Jeffree R, Drummond KJ, Gan H, Khasraw M (2018) Outcomes after second surgery for recurrent glioblastoma: a retrospective case–control study. J Neurooncol 137:409-415. https://doi.org/10.1007/s11060-017-2731-2

23. Fujita Y, Sasayama T, Tanaka K, Kyotani K, Nagashima H, Kohta M, Kimura H, Fujita A, Kohmura E (2019) DWI for monitoring the acute response of malignant gliomas to photodynamic therapy. Am J Neuroradiol 40:2045-2051. https://doi.org/10.3174/ajnr.A6300

24. Kanda Y (2013) Investigation of the freely available easy-to-use software 'EZR' for medical statistics.

391 Bone Marrow Transplant. 48:452-458. https:// doi.org/10.1038/bmt.2012.244.
392 25. Moan J, Berg K (1991) The photodegredation of porphyrins in cells can be used to estimate the lifetime
393 of singlet oxygen. Photochem Photobiol 53:549-553. https://doi.org/10.1111/j.1751-
394 1097.1991.tb03669.x
395 26. Stylli SS, Kaye AH (2006) Photodynamic therapy of cerebral glioma – A review Part I – A biological
396 basis. J Clin Neurosci 13:615-625. https://doi.org/10.1016/J.JOCN.2005.11.014
397 27. Henderson BW, Waldow SM, Mang TS, Potter WR, Malone PB, Dougherty TJ (1985) Tumor
398 destruction and kinetics of tumor cell death in two experimental mouse tumors following photodynamic
399 therapy. Cancer Res 45:572-576.
400 28. Fingar VH, Wieman TJ, Haydon PS (1997) The effects of thrombocytopenia on vessel stasis and
401 macromolecular leakage after photodynamic therapy using photofrin. Photochem Photobiol 66:513-517.
402 https://doi.org/10.1111/j.1751-1097.1997.tb03182.x
403 29. Ferrario A, von Tiehl KF, Rucker N, Schwarz MA, Gill PS, Gomer CJ (2000) Antiangiogenic treatment
404 enhances photodynamic therapy responsiveness in a mouse mammary carcinoma. Cancer Res 60:4066-
405 4069
406 30. Shumaker BP, Hetzel FW (1987) Clinical laser photodynamic therapy in the treatment of bladder
407 carcinoma. Photochem Photobiol 46:899-901. https://doi.org/10.1111/j.1751-1097.1987.tb04866.x
408 31. de Vree WJ, Essers MC, de Bruijn HS, Star WM, Foster JF, Sluiter W (1996) Evidence for an important
409 role of neutrophils in the efficacy of photodynamic therapy in vivo. Cancer Res 56:2908-2911.
410 32. Gollnick SO, Liu X, Owczarczak B, Musser DA, Henderson BW (1997) Altered expression of
411 interleukin 6 and interleukin 10 as a result of photodynamic therapy in vivo. Cancer Res 57:3904-3909.
412 33. Moseley ME, Cohen Y, Mintorovitch J, Chileuitt L, Shimizu H, Kucharczyk J, Wendland MF,
413 Weinstein PR (1990) Early detection of regional cerebral ischemia in cats: Comparison of diffusion- and
414 T2-weighted MRI and spectroscopy. Magn Reson Med 14:330-346.
415 https://doi.org/10.1002/mrm.1910140218
416 34. Ellingson BM, Abrey LE, Nelson SJ, Kaufmann TJ, Garcia J, Chinot O, Saran F, Nishikawa R,
417 Henriksson R, Mason WP, Wick W, Butowski N, Ligon KL, Gerstner ER, Colman H, de Groot J,
418 Chang S, Mellinghoff I, Young RJ, Alexander BM, Colen R, Taylor JW, Arrillaga-Romany I, Mehta A,
419 Huang RY, Pope WB, Reardon D, Batchelor T, Prados M, Galanis E, Wen PY, Cloughesy TF (2018)
420 Validation of postoperative residual contrast-enhancing tumor volume as an independent prognostic
421 factor for overall survival in newly diagnosed glioblastoma. Neuro Oncol 20:1240-1250.
422 https://doi.org/10.1093/neuonc/noy053
423 35. Huang Z, Hsu YC, Li LB, Wang LW, Song XD, Yow CMN, Lei X, Musani AI, Luo RC, Day BJ (2015)
424 Photodynamic therapy of cancer - Challenges of multidrug resistance. J Innov Opt Health Sci
425 8:1530002. https://doi.org/10.1142/S1793545815300025
426 36. Gołab J, Nowis D, Skrzycki M, Czeczot H, Baranczyk-Kuzma A, Wilczynski GM, Makowski M, Mroz
427 P, Kozar K, Kaminski R, Jalili A, Kopec' M, Grzela T, Jakobisiak M (2003) Antitumor effects of
428 photodynamic therapy are potentiated by 2-methoxyestradiol: A superoxide dismutase inhibitor. J Biol

Chem 278:407-414. https://doi.org/10.1074/jbc.M209125200

37. Broekgaarden M, Weijer R, van Gulik TM, Hamblin MR, Heger M (2015) Tumor cell survival pathways activated by photodynamic therapy: a molecular basis for pharmacological inhibition strategies. Cancer Metastasis Rev 34:643-690. https://doi.org/10.1007/s10555-015-9588-7

38. Agostinis P, Berg K, Cengel KA, Foster TH, Girotti AW, Gollnick SO, Hahn SM, Hamblin MR, Juzeniene A, Kessel D, Korbelik M, Moan J, Mroz P, Nowis D, Piette J, Wilson BC, Golab J (2011) Photodynamic therapy of cancer: An update. CA Cancer J Clin 61:250-281. https://doi.org/10.3322/caac.20114

39. Ghahe SS, Kosicki K, Wojewódzka M, Majchrzak BA, Fogtman A, Iwanicka-Nowicka R, Ciuba A, Koblowska M, Kruszewski M, Tudek B, Speina E (2021) Increased DNA repair capacity augments resistance of glioblastoma cells to photodynamic therapy. DNA Repair (Amst) 104:103136. https://doi.org/10.1016/j.dnarep.2021.103136

40. Thompson EM, Frenkel EP, Neuwelt EA (2011) The paradoxical effect of bevacizumab in the therapy of malignant gliomas. Neurology 76:87-93. https://doi.org/10.1212/WNL.0b013e318204a3af

41. van Dijken BRJ, van Laar PJ, Li C, Yan JL, Boonzaier NR, Price SJ, FCRS, van der Hoorn A (2019) Ventricle contact is associated with lower survival and increased peritumoral perfusion in glioblastoma. J Neurosurg 131:717-723. https://doi.org/10.3171/2018.5.JNS18340

42. Mistry AM, Kelly PD, Gallant JN, Mummareddy N, Mobley BC, Thompson RC, Chambless LB (2019) Comparative analysis of subventricular zone glioblastoma contact and ventricular entry during resection in predicting dissemination, hydrocephalus, and survival. Neurosurgery 85:E924-E932. https://doi.org/10.1093/neuros/nyz144

43. Mistry AM, Kelly PD, Thompson RC, Chambless LB (2018) Cancer dissemination, hydrocephalus, and survival after cerebral ventricular entry during high-grade glioma surgery: A meta-analysis. Neurosurgery 83:1119-1127. https://doi.org/10.1093/neuros/nyy202

44. Young JS, Gogos AJ, Pereira MP, Morshed RA, Li J, Barkovich MJ, Hervey-Jumper SL, Berger MS (2021) Effects of ventricular entry on patient outcome during glioblastoma resection. J Neurosurg. https://doi.org/10.3171/2020.7.jns201362

45. Elliott JP, Keles GE, Waite M, Temkin N, Berger MS (1994) Ventricular entry during resection of malignant gliomas: effect on intracranial cerebrospinal fluid tumor dissemination. J Neurosurg 80:834-839. https://doi.org/10.3171/jns.1994.80.5.0834

459 **Table 1** Patient characteristics

Characteristic	PDT (n = 30)
Age, years	
Median (range)	60.5 (23–85)
Sex, n (%)	
Male	16 (53)
Female	14 (47)
Preoperative Karnofsky Performance Status score	
Median (range)	80 (30–100)
Tumor locations, n (%)	
Frontal	14 (47)
Temporal	9 (30)
Parietal	4 (13)
Occipital	1 (3)
Insular	1 (3)
Basal ganglia	1 (3)
Laterality, n (%)	
Right	20 (67)
Left	10 (33)
Preoperative tumor volume, cm^3	
Median (range)	32.9 (2.2–140.0)
PDT	
Median (range)	14 (2–31)
Extent of resection, n (%)	
Gross total	23 (77)
Subtotal	5 (17)
Partial	2 (7)
Histopathology, n (%)	
Glioblastoma	26 (87)
Anaplastic astrocytoma	2 (7)
Anaplastic oligodendroglioma	2 (7)
Isocitrate dehydrogenase mutation status, n (%)	
Wild-type	25 (83)

Mutant	5 (17)
MGMT promoter methylation status, n (%)	
Methylated	15 (50)
Unmethylated	9 (30)
Unknown	6 (20)
MIB-1 index, %	
Median (range)	20 (10–80)

460 PDT, photodynamic therapy; MGMT, O^6-methylguanine-DNA methyltransferase

461 **Table 2** Tumor characteristics based on recurrence pattern after PDT

Characteristic	Local (n = 10)	Distant (n = 1)	Dissemination (n = 8)	None (n = 11)
Tumor locations, n (%)				
Frontal	3 (30)	1 (100)	4 (50)	6 (55)
Temporal	4 (40)	0 (0)	1 (13)	4 (36)
Parietal	2 (20)	0 (0)	1 (13)	1 (9)
Occipital	0 (0)	0 (0)	1 (13)	0 (0)
Insular	1 (10)	0 (0)	0 (0)	0 (0)
Basal ganglia	0 (0)	0 (0)	1 (13)	0 (0)
Laterality, n (%)				
Right	6 (60)	1 (100)	5 (63)	8 (73)
Left	4 (40)	0 (0)	3 (38)	3 (27)
Preoperative tumor volume, cm^3				
Median (range)	32.9 (10.9–108.7)	8.7	34.6 (2.2–102.9)	37.7 (3.6–140.0)
PDT				
Median (range)	12 (2–31)	9	15 (8–22)	15 (5–31)
Extent of resection, n (%)				
Gross total	9 (90)	1 (100)	5 (63)	8 (73)
Subtotal	1 (10)	0 (0)	3 (38)	1 (9)
Partial	0 (0)	0 (0)	0 (0)	2 (18)
Histopathology, n (%)				
Glioblastoma	10 (100)	1 (100)	7 (88)	8 (73)
Anaplastic astrocytoma	0 (0)	0 (0)	0 (0)	2 (18)
Anaplastic oligodendroglioma	0 (0)	0 (0)	1 (13)	1 (9)
Isocitrate dehydrogenase mutation status, n (%)				
Wild-type	10 (100)	1 (100)	6 (75)	8 (73)
Mutant	0 (0)	0 (0)	2 (25)	3 (27)
MGMT promoter methylation status, n (%)				
Methylated	6 (60)	1 (100)	3 (38)	5 (45)
Unmethylated	3 (30)	0 (0)	2 (25)	4 (36)
Unknown	1 (10)	0 (0)	3 (38)	2 (18)
MIB-1 index, %				

Median (range)	25 (10–70)	30	40 (10–80)	20 (10–25)

462 PDT, photodynamic therapy; MGMT, O^6-methylguanine-DNA methyltransferase

Figure Legends

Fig. 1 Axial diffusion-weighted imaging (DWI), T2-weighted FLAIR, and contrast-enhanced T1-weighted imaging (CE-T1WI) of a 49-year-old woman showing a contrast-enhancing tumor in the left frontal lobe (upper row of a). Post-PDT magnetic resonance (MR) images obtained on day 1 show complete resection of the contrast-enhancing lesion and hyperintense signal on DWI adjacent to the resection cavity wall (middle row of a). Follow-up MR images show local recurrence in the resection cavity wall of the primary tumor 22.5 months after surgery (lower row of a). DWI (left of b) and CE-T1WI (right of b) show the relationship between the hyperintense signal as the acute response and the recurrence site after PDT. The circle with the dotted line indicates the area without hyperintense signal on DWI as the acute response (left of b). The white arrow indicates the local recurrence site (right of b). The recurrence site is the area that does not show a hyperintense signal on DWI obtained on day 1 after PDT (b). The histopathological diagnosis was WHO grade IV glioblastoma, IDH wild-type. PDT, photodynamic therapy

Fig. 2 Axial diffusion-weighted imaging (DWI), T2-weighted FLAIR, and contrast-enhanced T1-weighted imaging (CE-T1WI) of a 67-year-old woman showing a contrast-enhancing tumor in the right temporal lobe (upper row of a). Post-PDT magnetic resonance (MR) images obtained on day 1 show complete resection of the contrast-enhancing lesion and hyperintense signal on DWI adjacent to the resection cavity wall (middle row of a). Follow-up MR images show local recurrence in the resection cavity wall of the primary tumor 7.7 months after surgery (lower row of a). DWI (left of b) and CE-T1WI (right of b) show the relationship of the hyperintense signal as the acute response with the recurrence site after PDT. The circle with the dotted line indicates the area without hyperintense signal on DWI as the acute response (left of b). The white arrow indicates the local recurrence site (right of b). The recurrence site is the area that does not show a hyperintense signal on DWI obtained on day 1 after PDT (b). The histopathological diagnosis was WHO grade IV glioblastoma, IDH wild-type. PDT, photodynamic therapy

Fig. 3 Axial diffusion-weighted imaging (DWI), T2-weighted FLAIR, and contrast-enhanced T1-weighted imaging (CE-T1WI) of a 40-year-old man showing a ring-enhancing tumor in the left frontal lobe (a–c). Post-PDT magnetic resonance (MR) images obtained on day 1 show complete resection of the contrast-enhancing lesion and hyperintense signal on DWI adjacent to the resection cavity wall (d–f). Follow-up MR images at 32.7 months after surgery show intact tumor tissue in the primary tumor bed (g–i) and distant recurrence in the left

frontal lobe (j–l). The histopathological diagnosis was WHO grade IV glioblastoma, IDH wild-type. PDT, photodynamic therapy

Fig. 4 Axial diffusion-weighted imaging (DWI), T2-weighted FLAIR, and contrast-enhanced T1-weighted imaging (CE-T1WI) of a 76-year-old man showing a ring-enhancing tumor in the left parietal lobe (a–c). Post-PDT magnetic resonance (MR) images obtained on day 1 show complete resection of the contrast-enhancing lesion and hyperintense signal on DWI adjacent to the resection cavity wall (d–f). Follow-up MR images at 1.4 months after surgery show intact tumor tissue in the primary tumor bed (g–i) and dissemination (j–l). The histopathological diagnosis was WHO grade IV glioblastoma, IDH wild-type. PDT, photodynamic therapy

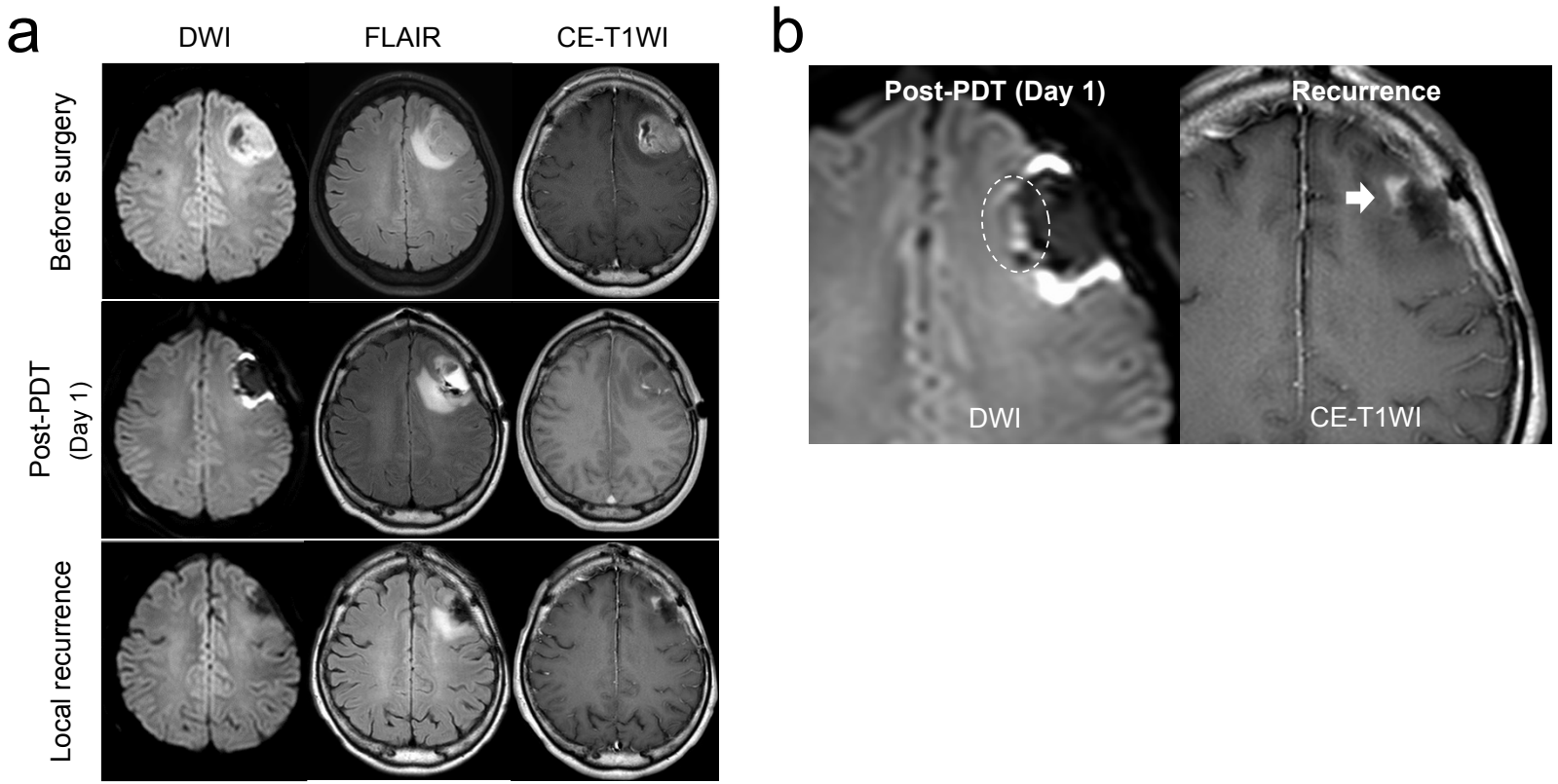
a
DWI
FLAIR
CE-T1WI
Before surgery
Post-PDT
(Day 1)
Local recurrence
b
Post-PDT (Day 1)
Recurrence
DWI
CE-T1WI

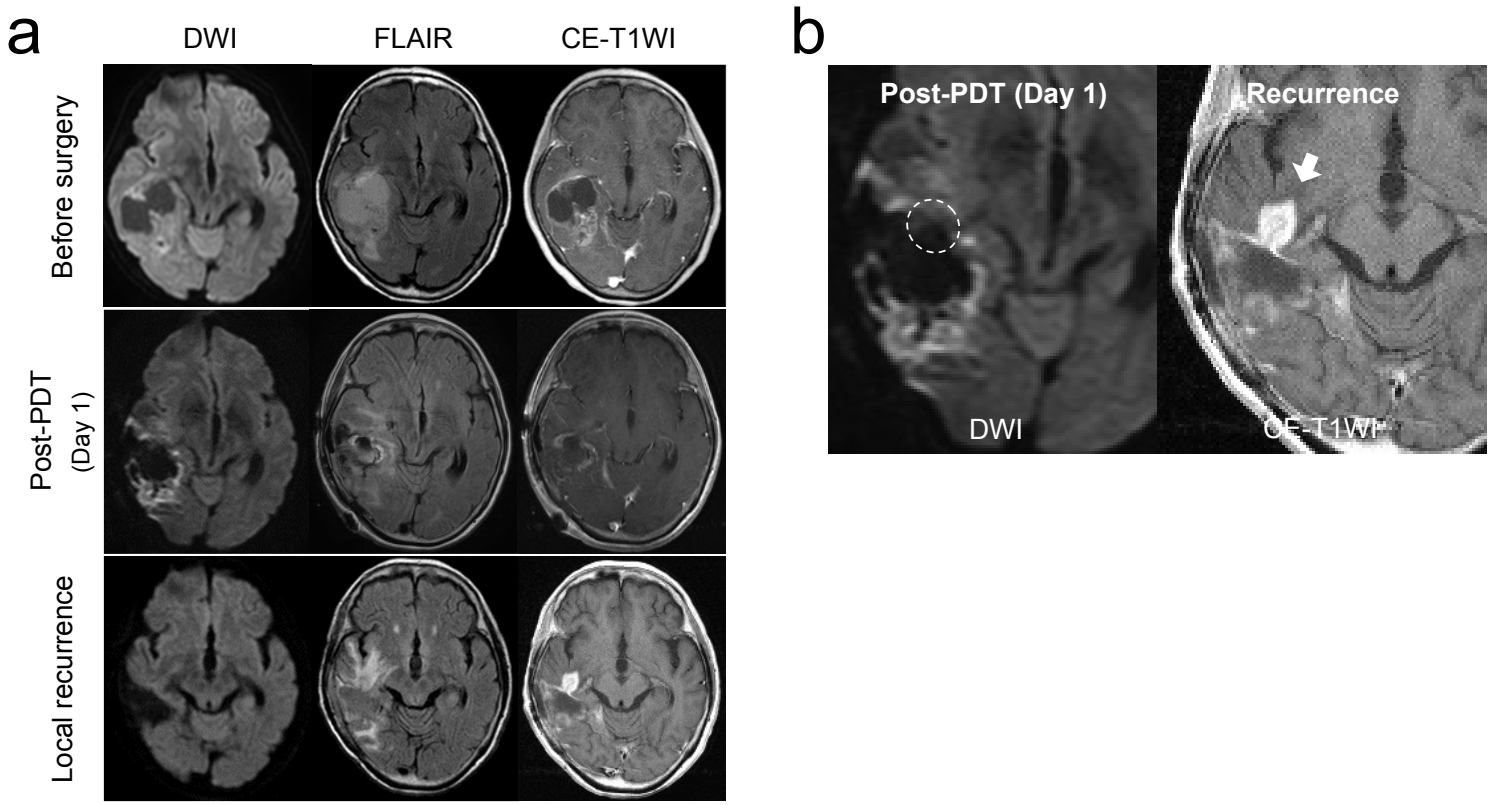
a
DWI
FLAIR
CE-T1WI
Before surgery
Post-PDT (Day 1)
Local recurrence
b
Post-PDT (Day 1)
Recurrence
DWI
CE-T1WI

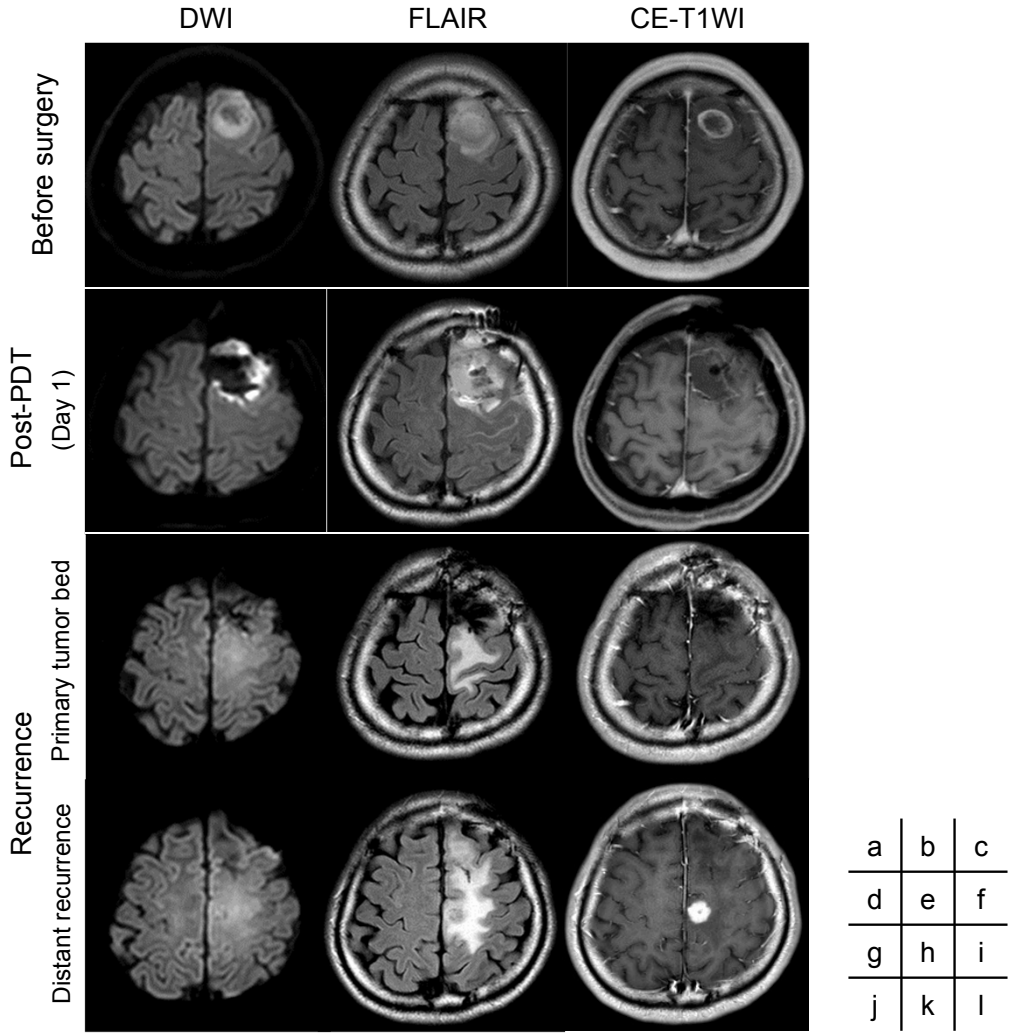

a	b	c
d	e	f
g	h	i
j	k	l

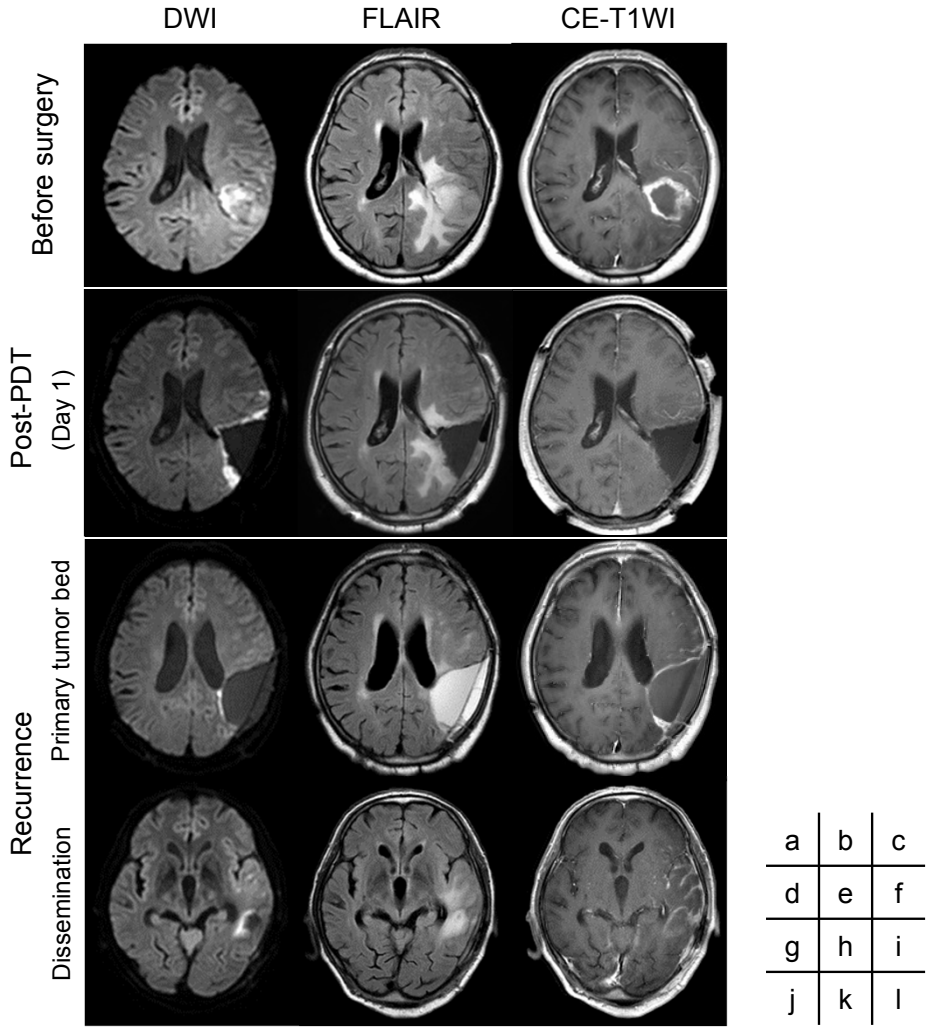

a	b	c
d	e	f
g	h	i
j	k	l

Supplementary Information for

Hyperintense signal on diffusion-weighted imaging for monitoring the acute response and local recurrence after photodynamic therapy in malignant gliomas

Yuichi Fujita*, Hiroaki Nagashima, Kazuhiro Tanaka, Mitsuru Hashiguchi, Tomoo Itoh, Takashi Sasayama

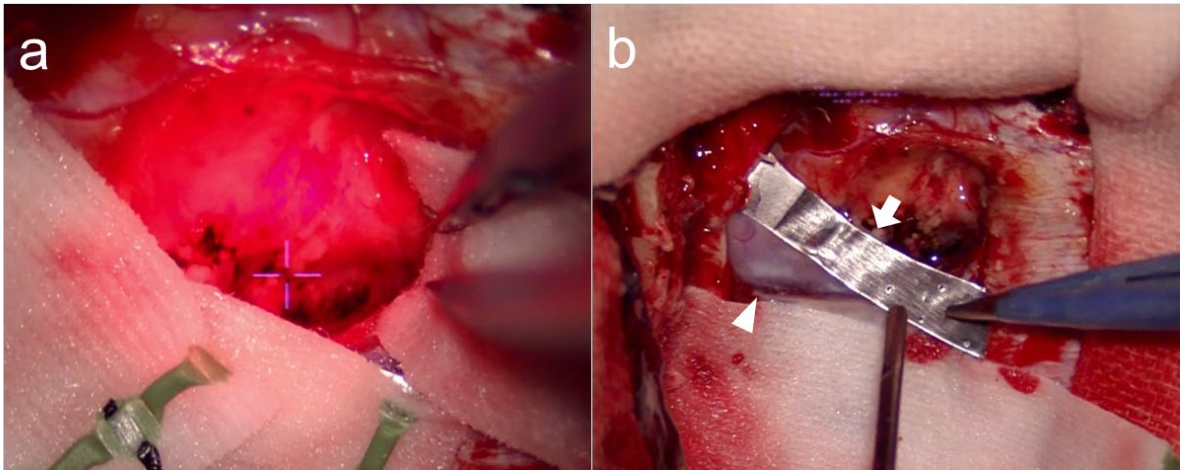

Supplementary Fig. 1 Intraoperative microscopic images during PDT. The resection cavity was irradiated with a semiconductor laser (a). The cross-hair indicates the focal point of the laser. The large blood vessel is protected by aluminum foil to avoid direct irradiation (b). PDT, photodynamic therapy

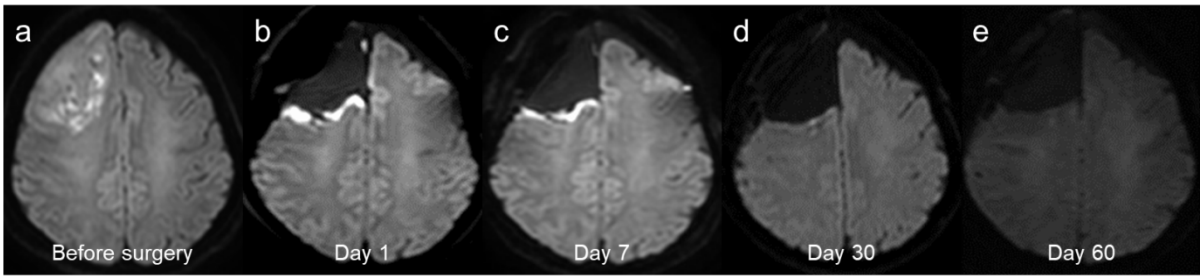

Supplementary Fig 2 Preoperative axial DWI of a representative case showing a mass lesion in the right frontal lobe (a). Postoperative DWI shows time-dependent changes after PDT (b–e). On day 1 after PDT, linear hyperintense signals were detected at the surface of the resected cavity (b). The hyperintense signals on DWI disappeared in about 30 days (c–e). DWI, diffusion-weighted imaging; PDT, photodynamic therapy

Supplementary Table 1 Characteristics of recurrent and non-recurrent patients

Characteristic	Recurrence (n = 19)	Non-recurrence (n = 11)	P Value
Age, years			0.12
Median (range)	62.0 (35–85)	48.0 (23–69)	
Sex, n (%)			0.47
Male	9 (47)	7 (64)	
Female	10 (53)	4 (36)	
Preoperative Karnofsky Performance Status score			0.09
Median (range)	70 (30–100)	90 (50–100)	
Tumor locations, n (%)			1.00
Frontal	8 (42)	6 (55)	
Temporal	5 (26)	4 (36)	
Parietal	3 (16)	1 (9)	
Occipital	1 (5)	0 (0)	
Insular	1 (5)	0 (0)	
Basal ganglia	1 (5)	0 (0)	
Laterality, n (%)			0.70
Right	12 (63)	8 (73)	
Left	7 (33)	3 (27)	
Preoperative tumor volume, cm^3			0.80
Median (range)	31.5 (2.2–108.7)	37.7 (3.6–140.0)	
PDT			0.62
Median (range)	12 (2–31)	15 (5–31)	
Extent of resection, n (%)			0.24
Gross total	15 (79)	8 (73)	
Subtotal	4 (21)	1 (9)	
Partial	0 (0)	2 (18)	
Histopathology, n (%)			0.13
Glioblastoma	18 (95)	8 (73)	
Anaplastic astrocytoma	0 (0)	2 (18)	
Anaplastic oligodendroglioma	1 (5)	1 (9)	
Isocitrate dehydrogenase mutation status, n (%)			0.33
Wild-type	17 (89)	8 (73)	
Mutant	2 (11)	3 (27)	
MGMT promoter methylation status, n (%)			0.68
Methylated	10 (53)	5 (45)	
Unmethylated	5 (26)	4 (36)	
Unknown	4 (21)	2 (18)	
MIB-1 index, %			0.01
Median (range)	30 (10–80)	20 (10–25)	

PDT, photodynamic therapy; MGMT, O^6-methylguanine-DNA methyltransferase

Supplementary Table 2 Characteristics of patients based on recurrence patterns

Characteristic	Local (n = 10)	Distant (n = 1)	Dissemination (n = 8)	P value
Age, years				0.22
Median (range)	61.0 (43–73)	40	68.0 (35–85)	
Sex, n (%)				0.24
Male	3 (30)	1 (100)	5 (63)	
Female	7 (70)	0 (0)	3 (38)	
Preoperative Karnofsky Performance Status score				0.59
Median (range)	70 (50–100)	90	70 (30–100)	
Tumor locations, n (%)				–
Frontal	3 (30)	1 (100)	4 (50)	
Temporal	4 (40)	0 (0)	1 (13)	
Parietal	2 (20)	0 (0)	1 (13)	
Occipital	0 (0)	0 (0)	1 (13)	
Insular	1 (10)	0 (0)	0 (0)	
Basal ganglia	0 (0)	0 (0)	1 (13)	
Laterality, n (%)				0.74
Right	6 (60)	1 (100)	5 (63)	
Left	4 (40)	0 (0)	3 (38)	
Preoperative tumor volume, cm^3				0.34
Median (range)	32.9 (10.9–108.7)	8.7	34.6 (2.2–102.9)	
PDT				0.54
Median (range)	12 (2–31)	9	15 (8–22)	
Extent of resection, n (%)				0.34
Gross total	9 (90)	1 (100)	5 (63)	
Subtotal	1 (10)	0 (0)	3 (38)	
Partial	0 (0)	0 (0)	0 (0)	
Histopathology, n (%)				0.50
Glioblastoma	10 (100)	1 (100)	7 (88)	
Anaplastic astrocytoma	0 (0)	0 (0)	0 (0)	
Anaplastic oligodendroglioma	0 (0)	0 (0)	1 (13)	
Isocitrate dehydrogenase mutation status, n (%)				0.23
Wild-type	10 (100)	1 (100)	6 (75)	
Mutant	0 (0)	0 (0)	2 (25)	
MGMT promoter methylation status, n (%)				0.76
Methylated	6 (60)	1 (100)	3 (38)	
Unmethylated	3 (30)	0 (0)	2 (25)	
Unknown	1 (10)	0 (0)	3 (38)	
MIB-1 index, %				0.65
Median (range)	25 (10–70)	30	40 (10–80)	

PDT, photodynamic therapy; MGMT, O^6-methylguanine-DNA methyltransferase; NaN, not a number

---

*Corresponding author. Department of Neurosurgery, Kobe University Graduate School of Medicine, 7-5-1 Kusunoki-cho, Chuo-ku, Kobe, Hyogo 650-0017, Japan; Email: fyuichi@med.kobe-u.ac.jp